Research Square

Preprints are preliminary reports that have not undergone peer review.
They should not be considered conclusive, used to inform clinical practice,
or referenced by the media as validated information.

Prenatal RYR1-related congenital myopathy presenting as first-trimester cystic hygroma with generalized subcutaneous edema: molecular characterization of a case and systematic synthesis of the prenatal phenotype spectrum

Ru Jia
Shenyang Women's and Children's Hospital
Xuan Zhou[2]
Liaoning Province Key Laboratory of Assisted Reproduction
Wenyue Liu
Shenyang Women's and Children's Hospital
Lei Yu
Shenyang Women's and Children's Hospital
Yuan Lyu
hawk.lv@163.com

Shenyang Women's and Children's Hospital

Research Article

Keywords: RYR1, congenital myopathy, cystic hygroma, fetal hydrops, fetal akinesia deformation sequence, whole-exome sequencing, prenatal diagnosis, genotype–phenotype correlation

Posted Date: November 19th, 2026

DOI: https://doi.org/10.21203/rs.3.rs-11587803/v1

License: This work is licensed under a Creative Commons Attribution 4.0 International License. Read Full License

Additional Declarations: No competing interests reported.

Abstract

Background

Biallelic *RYR1* variants can cause prenatally lethal disease but remain under-recognized in fetal cystic hygroma and hydrops. Genotype–phenotype and genotype–protein correlates of compound heterozygous disease are incompletely defined. We molecularly and histopathologically characterized a fetus with first-trimester cystic hygroma and generalized subcutaneous edema and contextualized the findings through a systematic synthesis of published prenatal *RYR1*-related cases.

Methods

A fetus with cystic hygroma and generalized subcutaneous edema at 13 + 6 weeks of gestation underwent trio whole-exome sequencing (WES) with Sanger segregation analysis; the diagnostic laboratory's ACMG/AMP classifications were retained without author reclassification. Fetal skeletal muscle was examined by hematoxylin–eosin (HE) histology with image-based quantification and by *RYR1* immunohistochemistry (IHC) with ImageJ-based quantification of the DAB-positive area fraction (%Area), using a gestational-age-matched control. We systematically identified published *RYR1*-related cases with documented prenatal phenotypes and synthesized seven core prenatal features across case-rows.

Results

The fetus carried compound heterozygous *RYR1* variants (NM_000540.3): a paternal nonsense variant, c.5623G > T p.(Glu1875*), classified by the diagnostic laboratory as likely pathogenic, and a maternal missense variant, c.5543T > C p.(Leu1848Pro), classified by the diagnostic laboratory as a variant of uncertain significance (VUS); both map to the Handle domain of the bridging solenoid. Histology showed immature myotubes with a 3.4-fold lower nuclear area fraction and extensive myofiber/myotube myolysis versus control. *RYR1* immunoreactivity retained a sarcoplasmic-reticulum pattern but was modestly reduced (%Area 91.90% ± 0.65% vs 96.41% ± 1.48%). The systematic synthesis (16 publications; 21 case-rows including the present case) identified contractures/arthrogryposis (76%), decreased fetal movement (67%), increased nuchal translucency/cystic hygroma (52%), and hydrops/effusions (48%) as the most frequent prenatal features; inheritance was predominantly autosomal recessive, and outcomes were almost invariably lethal or severely disabling.

Conclusions

The combination of first-trimester cystic hygroma with generalized subcutaneous edema and two *RYR1* variants in trans raises suspicion of *RYR1*-related congenital myopathy. The laboratory-reported likely pathogenic/VUS genotype does not establish a definitive molecular diagnosis. Retained but modestly reduced *RYR1* immunoreactivity does not resolve the pathogenicity of the missense variant or establish

channel dysfunction. *RYR1* merits inclusion in the genetic workup of euploid fetal cystic hygroma, hydrops, and reduced fetal movement; WES is an appropriate first-line test, with WGS reserved for suspected deep-intronic alleles.

1. Introduction

The *RYR1* gene (MIM 180901; chromosome 19q13.2) encodes RyR1, the principal Ca^{2+}-release channel of the skeletal-muscle sarcoplasmic reticulum (SR) [1]. The 5,038-amino-acid protomer assembles into a ~ 2.3-MDa homotetramer in which a cytoplasmic shell of α-helical solenoid repeats, an N-terminal β-trefoil, and SPRY domains overlies a membrane-embedded S1–S6 pore [2, 3]. Through mechanical coupling with the dihydropyridine receptor (CaV1.1), RyR1 converts sarcolemmal depolarization into the SR Ca^{2+} efflux that drives excitation–contraction coupling [4, 5].

RYR1-related disorders (*RYR1*-RD) span an unusually wide clinical continuum, from malignant hyperthermia susceptibility and central core disease to multiminicore disease, congenital fiber-type disproportion, centronuclear myopathy, and core-rod myopathy [6–11]. Whereas dominant variants cluster in three mutational hotspots, recessive variants are distributed along the entire gene, and most biallelic patients carry one truncating, splice-site, or in-frame-indel allele together with a missense allele [12–15]. Whether specific structural regions shape the severity of recessive disease remains an open question: a structure–genotype analysis implicated the bridging-solenoid (Bsol) region as the most frequently affected domain in recessive *RYR1*-RD, but confirmatory genotype–phenotype data at the severe prenatal end remain sparse.

Three further gaps complicate prenatal practice. First, although fetal akinesia deformation sequence (FADS) and lethal multiple pterygium syndrome (LMPS) are established prenatal manifestations of biallelic *RYR1* disease [16, 17], and large fetal-akinesia cohorts confirm *RYR1* as a recurrent contributor [18, 19], *RYR1* is rarely considered in the workup of euploid fetal cystic hygroma or hydrops, which conventionally prioritizes lymphatic-dysplasia, cardiac, and hematological etiologies. Second, the protein-expression correlates of compound heterozygous loss-of-function/missense genotypes are poorly documented, leaving the diagnostic value of muscle IHC in this setting undefined. Third, deep-intronic *RYR1* alleles escape exome capture, and the respective roles of WES and WGS in prenatal diagnosis are not standardized.

We therefore performed a molecular, histopathological, and immunohistochemical characterization of a fetus presenting at 13 + 6 weeks with cystic hygroma and generalized subcutaneous edema and compound heterozygous *RYR1* variants of unresolved combined clinical significance, and systematically synthesized the published prenatal phenotype spectrum of molecularly confirmed *RYR1*-RD to delineate characteristic features and genotypic correlates.

2. Materials and methods

2.1. Study design

This study combines a case-anchored clinicopathological and molecular analysis with a systematic synthesis of published prenatal *RYR1*-RD cases. The study was approved by the Medical Ethics Committee of Shenyang Women's and Children's Hospital (approval no. PJ-SC-2026-050; approval letter dated 28 October 2026). The requirement for informed consent to participate was waived by the committee.

2.2. Genetic testing and variant classification

Genomic DNA was extracted from the fetal abortus (products of conception) and parental peripheral blood. Trio whole-exome sequencing was performed by target capture and high-throughput sequencing, covering the exonic regions (± 25 bp) of approximately 20,000 genes together with the mitochondrial genome; the proband achieved a mean sequencing depth of 213.25× with 99.90% target coverage (98.75% of bases at > 30×). Reads were aligned to the human reference genome (GRCh37/hg19), and variants were called and annotated with an in-house bioinformatics pipeline. Variants were prioritized by phenotypic relevance (cystic hygroma, subcutaneous edema, reduced fetal movement), compatibility with autosomal-recessive inheritance, and population allele frequency < 1%. Candidate variants were confirmed by Sanger sequencing in the fetus and both parents. Variant classifications and evidence codes were taken from the updated diagnostic laboratory report, which applied ACMG/AMP guidelines [20]; no author reclassification was performed. The report cited internal functional evidence (PS3_Supporting) for the missense variant, but the underlying assay methods and results were not provided for independent assessment. This evidence is reported as a laboratory assessment, not as functional testing performed in the present study.

2.3. RYR1 immunohistochemistry

Formalin-fixed, paraffin-embedded fetal skeletal muscle from the proband and a gestational-age-matched control fetus (a 14-week fetus following early fetal demise, i.e., a missed abortion) was stained with a mouse monoclonal anti-RYR1 antibody (clone 1B4E12; catalog no. AWA04584; Abiowell Biotechnology; immunogen corresponding to human RYR1 residues 4942–5038; used at a 1:100 dilution) using a standard avidin–biotin–peroxidase protocol with 3,3'-diaminobenzidine (DAB) and hematoxylin counterstaining, and imaged at ×400 (40× objective, 10× eyepiece). The DAB-positive area fraction (%Area) was quantified with ImageJ (NIH) by color separation and thresholding, expressed as the percentage of DAB-positive area within the total tissue area, in three representative fields per specimen.

2.4. Histology and image-based quantification

HE-stained skeletal-muscle sections (proband and control) were imaged at ×100. Each image was divided into a 3×3 tile grid; after white-point correction, hematoxylin and eosin channels were separated by color deconvolution [21], and a single pooled Otsu threshold [22] segmented hematoxylin-positive (nuclear) and low-optical-density (pale/myolytic) areas. Nuclear and pale area fractions were computed per tile relative to tissue area.

2.5. Literature search and data synthesis

PubMed was searched for molecularly confirmed *RYR1*-related disease with prenatal phenotypes (terms: "*RYR1*" AND "fetal"/"prenatal"/"fetal akinesia"/"multiple pterygium"/"hydrops"/"cystic hygroma"; last search October 21, 2026). Reports were eligible if they described at least one fetus or neonate with (likely)

pathogenic *RYR1* variant(s) and documented prenatal findings; reports documenting only fetal akinesia without further phenotypic detail were excluded from the tabulated synthesis. For each case or family we extracted ethnicity/consanguinity, variant(s) and zygosity, inheritance, gestational age at diagnosis, seven core prenatal features (increased nuchal translucency/cystic hygroma; hydrops/effusions; decreased fetal movement; contractures/arthrogryposis multiplex congenita (AMC); pterygia; polyhydramnios; pulmonary hypoplasia), additional findings, and outcome. Features not mentioned in a source were recorded as "not reported" (NR); frequencies therefore represent minimum estimates.

2.6. Statistical analysis

Given the single-case design (three IHC fields or nine HE tiles from one specimen per group), all quantitative results are reported descriptively as mean ± standard deviation; no inferential testing was performed, as field-level replicates from one biological specimen do not constitute independent observations.

3. Results

3.1. Clinical and prenatal imaging findings

A 39-year-old Chinese woman, gravida 5, para 1, presented at 14 weeks of gestation. Her obstetric history comprised two early spontaneous abortions (II-1, II-2), one healthy child (II-3), and one previous pregnancy terminated for an affected fetus (II-4) (Fig. 1A). The couple was non-consanguineous and healthy, with no family history of neuromuscular disease or malignant hyperthermia. Ultrasound at 13 + 6 weeks revealed a septated cystic hygroma measuring 25 × 29 × 12 mm, without detectable internal blood flow on color Doppler, together with generalized subcutaneous edema up to 4 mm thick (nuchal translucency not formally measured); the ductus venosus a-wave was absent or reversed. Three-dimensional imaging showed a fixed, flexed posture of both lower limbs (Fig. 1B). The fetus was singleton and live (fetal heart rate 155 bpm), with biometry appropriate for gestational age (crown–rump length 7.8 cm, biparietal diameter 2.3 cm, femur length 1.2 cm), grossly normal intracranial anatomy, and an intact abdominal wall. Fetal karyotyping and chromosomal microarray analysis were not performed. After genetic counseling, the pregnancy was terminated at 14 + 3 weeks of gestation. Postmortem autopsy was not performed.

3.2. Molecular characterization

Trio-WES identified two heterozygous *RYR1* variants (NM_000540.3) in the fetus, confirmed by Sanger sequencing to be in trans: c.5623G > T p.(Glu1875*) (exon 35; chr19:38979892, GRCh37), inherited from the heterozygous father, and c.5543T > C p.(Leu1848Pro) (exon 34; chr19:38976838, GRCh37), inherited from the heterozygous mother; both parents are asymptomatic carriers (Fig. 1).

The nonsense variant introduces a premature termination codon at residue 1,875, truncating 63% of the protein including the entire transmembrane pore, and the transcript is predicted to undergo nonsense-mediated mRNA decay (loss of function). The updated diagnostic laboratory report classified c.5623G > T, p.(Glu1875*), as likely pathogenic, citing PVS1 and PM2_Supporting. The missense variant replaces a

conserved leucine with proline within the Handle domain (residues 1,651–2,145) of the RyR1 bridging solenoid. The laboratory classified c.5543T > C, p.(Leu1848Pro), as a variant of uncertain significance (VUS), citing PS3_Supporting, PM2_Supporting, PM3, and PP3 under the ACMG/AMP framework [20]. PS3_Supporting was attributed in the report to internal functional experiments indicating impaired gene function; the experimental methods and results were not provided, so this evidence could not be independently assessed. These laboratory classifications were retained without author upgrading, and the report's overall result was inconclusive. The likely pathogenic/VUS genotype therefore remains a candidate explanation rather than a definitive molecular diagnosis. Neither variant was listed in ClinVar at the time of analysis, and both were absent from population databases (gnomAD v2.1.1 exomes, 1000 Genomes, ESP6500 and ExAC). In silico predictions supported deleteriousness of the missense substitution (SIFT, PolyPhen-2 and PROVEAN deleterious; CADD 25.5; REVEL 0.868), and the nonsense variant had a CADD score of 37.0. No other (likely) pathogenic variants relevant to the phenotype were detected, WES-based copy-number analysis was negative, and no reportable ACMG secondary-findings variants were identified.

3.3. Histopathology and RYR1 protein expression

HE-stained sections of the proband's skeletal muscle showed small, immature myotubes with sparse nuclei and extensive pale, structure-poor areas consistent with myofiber/myotube myolysis (Fig. 2A, B). Image-based quantification supported the visual impression (Fig. 2C): the hematoxylin-positive nuclear area fraction was markedly lower in the proband than in the control (7.5% ± 1.5% vs 25.6% ± 6.4% of tissue area; 3.4-fold lower), whereas the low-optical-density pale fraction was higher (93.3% ± 1.3% vs 70.6% ± 5.1%; 1.32-fold higher).

RYR1 immunoreactivity was detected in the sarcoplasm of fetal myotubes in both the proband and the control, with a granular cytoplasmic distribution consistent with SR localization (Fig. 2D, E). The DAB-positive area fraction was slightly lower in the proband than in the control (91.90% ± 0.65% vs 96.41% ± 1.48%; relative reduction ≈ 4.7%; Fig. 2F), indicating retained but modestly reduced RYR1 protein expression.

3.4. Systematic synthesis of the prenatal RYR1 phenotype spectrum

Sixteen publications met the inclusion criteria, yielding—together with the present case—21 case-rows for synthesis (Table 1; full dataset in Additional file 1: Table S1) [16, 17, 23–36]. Two additional reports were excluded because only fetal akinesia was documented [37, 38]. The present case is included as a clinically suspected, molecularly unresolved anchor case, not as an additional molecularly confirmed *RYR1*-RD diagnosis.

Table 1
Representative prenatal *RYR1*-related cases and the present suspected case.

Reference	RYR1 variant(s); zygosity	Inheritance	GA at diagnosis	Key prenatal findings	Outcome
Romero et al., 2003 [16]	Missense variants in 3/6 families (cDNA not specified)	AR (2) / AD (1)	IUFD 31 and 32 wk	Fetal akinesia with CCD; arthrogryposis, hip dislocation, kyphoscoliosis in liveborn	2 IUFD; 5 severe neonatal
McKie et al., 2014 (MPS001) [17]	c.6721C > T p. (Arg2241*); homozygous	AR	12 + 6 wk	NT 9 mm, cystic hygroma, akinesia, contractures, elbow/knee pterygia, lung hypoplasia	TOP
McKie et al., 2014 (MPS002) [17]	c.2097_2123del p. (Glu699_Gly707del); homozygous	AR	18 wk	Large cystic hygroma, subcutaneous edema, ascites, pleural + pericardial effusions, fixed joint flexion, cleft palate	TOP (19 wk)
McKie et al., 2014 (MPS003) [17]	c.7043delGAG p. (Glu2347del); homozygous	AR	23 + 3 wk	Cystic hygroma, hydrothorax, reduced fetal movement, multi-joint contractures, multi-site webbing, pulmonary hypoplasia	TOP
Kariminejad et al., 2016 (Case 1) [27]	c.4567A > C p. (Thr1523Pro) + c.9851G > A p. (Trp3284*); compound het	AR	18 wk	Cystic hygroma, pleural effusion, ascites, reduced fetal movement, contractures, elbow/knee webbing, club feet	TOP
Kariminejad et al., 2016 (Case 2) [27]	Same family as Case 1; compound het	AR	12 wk	Cystic hygroma with subcutaneous edema of skull/thorax/abdomen	Abortion (13 wk)
Meier et al., 2017 [24]	c.9686-1G > C (splice); homozygous	AR	24 wk	Hydrops fetalis, reduced fetal movement, flexion contractures, clubfeet, elbow pterygia, muscle hypoplasia incl. diaphragm	IUFD
Zhao et al., 2022 (II-5) [28]	c.2682G > C p. (Ile860_Pro894del) + c.12572G > A p. (Arg4191His); compound het	AR	25 wk	NT 8.8 mm, hand clenching, adducted thumb, polyhydramnios, subcutaneous edema, fetal immobility	TOP (28 wk)

Reference	RYR1 variant(s); zygosity	Inheritance	GA at diagnosis	Key prenatal findings	Outcome
Hou et al., 2024 [25]	c.538-33C > A (intron 6); heterozygous	Uncertain	12 + 4 wk	NT 7.22 mm, generalized edema, abdominal fluid, bilateral pleural effusions, fixed hand posture	TOP
Jackson et al., 2024 [23]	c.1266_1267delinsTT p.(Lys423*) + c.8171_8173delinsGG p.(Glu2724Glyfs*22); compound het	AR	12 + 1 wk	NT 9.1 mm, large cystic hygroma, hydrops (ascites, pleural effusions, skin edema), talipes, akinesia, multiple pterygia	IUFD (26 + 6 wk)
Wang et al., 2026 (II-1, II-4) [30]	Exon 94–97 deletion + deep-intronic c.4934 + 25G > A; compound het	AR	12 wk	Cystic hygroma, absent fetal movement, fixed limbs, foot deformity	TOP
Present case	c.5623G > T p.(Glu1875*) + c.5543T > C p.(Leu1848Pro); compound het	**AR**	**13 + 6 wk**	**Cystic hygroma with generalized subcutaneous edema**	**TOP**

 Hou et al.: the article title states "homozygous", but the main text reports both genotyped fetuses as heterozygous for c.538-33C > A; the authors concluded the heterozygous variant may contribute to hydrops. AR = autosomal recessive; AD = autosomal dominant; GA = gestational age; NT = nuchal translucency; IUFD = intrauterine fetal demise; TOP = termination of pregnancy; het = heterozygous; CCD = central core disease. For the present case, AR denotes the inheritance model under consideration, not a confirmed causal diagnosis; the maternal missense variant remains a VUS. The complete 21-row dataset is provided in Additional file 1: Table S1.

Across the 21 case-rows (Fig. 3), the most frequently reported prenatal features were contractures/AMC (16/21, 76%), decreased or absent fetal movement (14/21, 67%), increased nuchal translucency/cystic hygroma (11/21, 52%), and hydrops/effusions (10/21, 48%); pterygia (7/21, 33%), polyhydramnios (7/21, 33%), and pulmonary hypoplasia (5/21, 24%) were less frequently reported. Inheritance was predominantly autosomal recessive; exceptions included de novo heterozygous variants [32, 36], a heterozygous in-frame deletion for which additional genetic contributors were postulated [35], and a heterozygous intronic variant reported as contributing to fetal hydrops [25]. Outcomes were severe in nearly all cases—termination of pregnancy, intrauterine demise, or neonatal/infant death—with survival with severe disability in a minority [26, 31]. Cystic hygroma or increased NT was documented as early as 12–13 + 6 weeks in several case-rows [17, 27, 30], including the present case.

The complete feature-frequency summary is provided in Additional file 1: Table S2.

4. Discussion

4.1. Principal findings

This study combines molecular, histopathological, and protein-expression characterization of a fetus with first-trimester cystic hygroma and generalized subcutaneous edema and compound heterozygous *RYR1* variants classified as likely pathogenic and VUS, with a systematic synthesis of the published prenatal phenotype spectrum. Three findings emerge: (i) a predicted loss-of-function plus missense genotype in the bridging-solenoid domain co-occurred with severe prenatal abnormalities and retained—but modestly reduced—*RYR1* protein expression, without establishing causality; (ii) cystic hygroma and hydrops are recurrent, early, and under-appreciated features of prenatal *RYR1*-RD; and (iii) the genetic workup of euploid fetal cystic hygroma/hydrops rarely includes *RYR1*, despite actionable implications for recurrence risk and carrier management.

4.2. Contribution to the mechanistic understanding of biallelic RYR1 disease

The present genotype—a paternal nonsense allele (p.(Glu1875*)) in trans with a maternal missense allele (p.(Leu1848Pro))—matches the most common mutational configuration in recessive *RYR1*-RD, reported in approximately 61.5% of biallelic cases [13], and conforms to the observation that genotypes including at least one loss-of-function allele associate with greater severity [13, 14]. Both variants map to the Handle domain within the bridging solenoid, the region most frequently affected by recessive variants (84% in a structure–genotype analysis) and linked to severe phenotypes [39]. These structural parallels motivate a hypothesis that the present genotype could affect tetramer assembly or allosteric coupling. However, neither biallelic functional disruption nor expression of the proposed full-length missense product was demonstrated in this study, and the maternal variant remains a VUS.

This domain-specific mechanism can be situated within the broader landscape of *RYR1* channel dysfunction. Variants in the pore-lining S6 helix and the C-terminal transmembrane assembly cause loss of function by a more direct route: the in-frame pore deletion p.(Phe4923_Phe4924del), identified in two brothers with lethal fetal akinesia, was shown functionally to form channels that are not activated by Ca^{2+} and do not conduct Ca^{2+} at the single-channel level [35]; the C-terminal transmembrane variant p.(Ile4898Thr) causes lethal core-rod myopathy [36]; and dominant CCD variants likewise cluster in the C-terminal transmembrane exons 101–102 [15]. These pore/transmembrane lesions illustrate established mechanisms of impaired Ca^{2+} conductance; an allosteric mechanism for the present genotype remains a hypothesis rather than a demonstrated parallel. This contrasts sharply with the dominant malignant-hyperthermia and central-core-disease variants, which cluster in three mutational hotspots (N-terminal, residues ~ 35–614; central, ~ 2163–2458; C-terminal, ~ 4550–4940) and act by gain of function: the mutant channel is hypersensitive to activators and/or leaks Ca^{2+} at rest, as illustrated at atomic resolution by the central-region Y522S variant, which remodels a hydrophobic network to preactivate the channel and increase its Ca^{2+}-activation potency [6, 41]. Because a single leaky protomer within the tetramer is sufficient to dysregulate gating, such variants are dominant and typically produce triggered (malignant hyperthermia) or chronic myopathic (central core disease) phenotypes rather than prenatal lethality. These published

examples outline a mechanistic spectrum from loss of function to gain-of-function leak; the functional position of the present genotype cannot be established from the available data.

4.3. Cystic hygroma and hydrops as first-trimester neuromuscular signals

Our synthesis shows that increased NT/cystic hygroma (52%) and hydrops/effusions (48%) are reported in roughly half of prenatal *RYR1*-RD case-rows and can precede recognition of akinesia or contractures; several cases, including ours, were evident at 12–13 + 6 weeks [17, 27, 30]. In the present case, three-dimensional imaging additionally documented a fixed posture of both lower limbs, an early sonographic sign of fetal akinesia, and the ductus venosus a-wave was absent or reversed—a Doppler sign of the hemodynamic compromise that accompanies the fluid-accumulation phenotype. A mechanistic link is biologically plausible: fetal movement is required for normal lymphatic development and interstitial-fluid homeostasis, so severe congenital myopathy with early akinesia may secondarily produce nuchal fluid accumulation and hydrops, as proposed for other fetal-akinesia genes [18]. These observations extend—rather than overturn—current practice: in euploid fetuses with cystic hygroma or hydrops, neuromuscular etiologies, including *RYR1*, deserve a place alongside lymphatic-dysplasia and cardiac workups.

Figure 4. Proposed disease mechanism and variant locations. The diagram links biallelic *RYR1* disruption to fetal fluid accumulation and maps the present variants. Left: schematic of the RyR1 homotetramer in the sarcoplasmic-reticulum membrane; the Handle/bridging-solenoid (Bsol) domain (amino acids 1651–2145) is highlighted, and the positions of the paternal nonsense variant p.(Glu1875*) and the maternal missense variant p.(Leu1848Pro) are indicated. Right: proposed mechanistic cascade—biallelic *RYR1* disruption impairs excitation–contraction coupling, causing fetal akinesia; the resulting loss of fetal movement secondarily impairs lymphatic drainage and interstitial-fluid homeostasis, producing cystic hygroma, generalized subcutaneous edema, or hydrops. The cascade is a hypothetical disease model, not a demonstrated functional consequence of the present variants; the maternal p.(Leu1848Pro) variant remains a VUS, and biallelic *RYR1* disruption has not been established in this fetus.

4.4. Genotype–protein correlation and the diagnostic limits of immunohistochemistry

RYR1 immunoreactivity in the proband retained an SR-consistent sarcoplasmic pattern, and the DAB-positive area fraction was only modestly lower than control (≈ 4.7% relative reduction). One possible interpretation is that the p.(Glu1875*) transcript undergoes nonsense-mediated decay while the p.(Leu1848Pro) allele, if expressed, produces a full-length antibody-detectable protein. Neither transcript fate nor allele-specific protein expression or dysfunction was measured. The antibody epitope (residues 4942–5038) lies C-terminal to both variants and is therefore retained in the full-length p.(Leu1848Pro) product but would be absent from any truncated p.(Glu1875*) protein (residues 1–1874). The IHC findings describe immunoreactivity, not channel function, and do not resolve the pathogenicity of the missense VUS or establish a molecular diagnosis. Independent functional assays (e.g., calcium-release measurements) would be needed to assess channel dysfunction directly.

4.5. Therapeutic outlook

No disease-modifying therapy exists for prenatal *RYR1*-RD. Nevertheless, mechanistic work in postnatal models offers a conceptual frame: stabilization of leaky RyR1 channels with Rycal compounds improved muscle function in a murine model of recessive *RYR1*-RD [40], and allele-specific strategies are being explored for dominant disease. For the lethal prenatal end of the spectrum, the realistic near-term benefit of molecular diagnosis lies in reproductive options—early prenatal diagnosis and preimplantation genetic testing—rather than in utero therapy; any future intervention would require functional rescue of biallelic channel deficiency during fetal myogenesis. For the present family, causal uncertainty must be made explicit in reproductive counseling; the VUS should not be treated as an established disease-causing allele.

4.6. Limitations

This is a single anchor case; the systematic synthesis mitigates, but does not eliminate, the limited generalizability. IHC and HE quantifications are descriptive, based on three fields or nine tiles from one specimen per group, and no inferential statistics were applied. The maternal missense variant remains a VUS, so the likely pathogenic/VUS genotype does not establish a definitive molecular diagnosis. Although the updated laboratory report cited PS3_Supporting from internal functional experiments, the assay methods and results were not provided for independent assessment. No independent channel-function validation was performed in this study, and the histological and IHC findings do not resolve this uncertainty. Literature frequencies are minimum estimates because unreported features were scored as not reported, and aggregate reports limited per-individual resolution.

5. Conclusions

A fetus with first-trimester cystic hygroma and generalized subcutaneous edema carried compound heterozygous *RYR1* variants in the bridging-solenoid domain: a paternal nonsense allele (c.5623G > T, p.(Glu1875*)) classified by the diagnostic laboratory as likely pathogenic, and a maternal missense allele (c.5543T > C, p.(Leu1848Pro)) classified as a VUS. Histology showed myotube developmental impairment and myolysis, with retained but modestly reduced *RYR1* immunoreactivity. These observations raise suspicion of *RYR1*-related congenital myopathy but do not establish the causal role of the missense variant or a definitive molecular diagnosis. Systematic synthesis identifies contractures, decreased fetal movement, increased NT/cystic hygroma, and hydrops as characteristic reported prenatal features of *RYR1*-RD; the present unresolved case is included descriptively. *RYR1* merits inclusion in the genetic workup of euploid fetuses with cystic hygroma, hydrops, or reduced fetal movement; WES is first-line, with WGS reserved for suspected deep-intronic alleles. Recurrence-risk counseling in this family must remain conditional on establishing causality, and carrier-management recommendations must reflect the unresolved variant interpretation.

Abbreviations

AMC
arthrogryposis multiplex congenita

Bsol
bridging solenoid
CCD
central core disease
DAB
3,3'-diaminobenzidine
FADS
fetal akinesia deformation sequence
HE
hematoxylin–eosin
IHC
immunohistochemistry
LMPS
lethal multiple pterygium syndrome
NR
not reported
NT
nuchal translucency
RYR1-RD
RYR1-related disorder
SR
sarcoplasmic reticulum
VUS
variant of uncertain significance
WES
whole-exome sequencing
WGS
whole-genome sequencing.

Declarations

Ethics approval and consent to participate:

All methods and experiments involving human participants, human data, or human samples were performed in accordance with the Declaration of Helsinki and relevant guidelines and regulations. The study was approved by the Medical Ethics Committee of Shenyang Women's and Children's Hospital, Shenyang, China (approval no. PJ-SC-2026-050; approval letter dated 28 October 2026). The requirement for informed consent to participate was waived by the Medical Ethics Committee of Shenyang Women's and Children's Hospital.

Consent for publication:

Written informed consent for publication of their personal or clinical details, together with any identifying images, was obtained from all adult participants and from the parents or legal guardians of the fetus.

Competing interests:

The authors declare no competing interests.

Funding:

This work was supported by the General Project of Natural Science Foundation of Liaoning Province (grant number: 2025-MS-362).

Author Contribution

Ru Jia performed the majority of the experiments, processed the study data, and drafted the manuscript. Xuan Zhou conducted the literature search and revised the manuscript. Wenyue Liu performed experiments. Lei Yu performed experiments, organized the data, and conducted statistical analyses. Yuan Lyu designed the methodology, acquired funding, and supervised the research.All authors reviewed the manuscript.

Data Availability

All data supporting the findings of this study are available within the paper and its Supplementary Information.

References

1. Phillips MS, Fujii J, Khanna VK, DeLeon S, Yokobata K, de Jong PJ, et al. The structural organization of the human skeletal muscle ryanodine receptor (RYR1) gene. Genomics. 1996;34(1):24–41. 10.1006/geno.1996.0238.
2. Clarke OB, Hendrickson WA. Structures of the colossal RyR1 calcium release channel. Curr Opin Struct Biol. 2016;39:144–52. 10.1016/j.sbi.2016.09.002.
3. Melville Z, Kim K, Clarke OB, Marks AR. High-resolution structure of the membrane-embedded skeletal muscle ryanodine receptor. Structure. 2022;30(1):172–e803. 10.1016/j.str.2021.08.001.
4. Lanner JT, Georgiou DK, Joshi AD, Hamilton SL. Ryanodine receptors: structure, expression, molecular details, and function in calcium release. Cold Spring Harb Perspect Biol. 2010;2(11):a003996. 10.1101/cshperspect.a003996.
5. Meissner G. The structural basis of ryanodine receptor ion channel function. J Gen Physiol. 2017;149(12):1065–89. 10.1085/jgp.201711878.

6. Robinson R, Carpenter D, Shaw MA, Halsall J, Hopkins P. Mutations in RYR1 in malignant hyperthermia and central core disease. Hum Mutat. 2006;27(10):977–89. 10.1002/humu.20356.
7. Lillis S, Abbs S, Mueller CR, Muntoni F, Jungbluth H. Clinical utility gene card for: central core disease. Eur J Hum Genet. 2012;20(2). 10.1038/ejhg.2011.179.
8. Ogasawara M, Nishino I. A review of core myopathy: central core disease, multiminicore disease, dusty core disease, and core-rod myopathy. Neuromuscul Disord. 2021;31(10):968–77. 10.1016/j.nmd.2021.08.015.
9. Snoeck M, van Engelen BG, Küsters B, Lammens M, Meijer R, Molenaar JP, et al. RYR1-related myopathies: a wide spectrum of phenotypes throughout life. Eur J Neurol. 2015;22(7):1094–112. 10.1111/ene.12713.
10. Lawal TA, Todd JJ, Witherspoon JW, Bönnemann CG, Dowling JJ, Hamilton SL, et al. Ryanodine receptor 1-related disorders: an historical perspective and proposal for a unified nomenclature. Skelet Muscle. 2020;10(1):32. 10.1186/s13395-020-00243-4.
11. Lawal TA, Todd JJ, Meilleur KG. Ryanodine receptor 1-related myopathies: diagnostic and therapeutic approaches. Neurotherapeutics. 2018;15(4):885–99. 10.1007/s13311-018-00677-1.
12. Clarke NF, Waddell LB, Cooper ST, Perry M, Smith RL, Kornberg AJ, et al. Recessive mutations in RYR1 are a common cause of congenital fiber type disproportion. Hum Mutat. 2010;31(7):E1544–50. 10.1002/humu.21278.
13. Klein A, Lillis S, Munteanu I, Scoto M, Zhou H, Quinlivan R, et al. Clinical and genetic findings in a large cohort of patients with ryanodine receptor 1 gene-associated myopathies. Hum Mutat. 2012;33(6):981–8. 10.1002/humu.22056.
14. Amburgey K, Bailey A, Hwang JH, Tarnopolsky MA, Bönnemann CG, Medne L, et al. Genotype-phenotype correlations in recessive RYR1-related myopathies. Orphanet J Rare Dis. 2013;8:117. 10.1186/1750-1172-8-117.
15. Zhou H, Jungbluth H, Sewry CA, Feng L, Bertini E, Bushby K, et al. Molecular mechanisms and phenotypic variation in RYR1-related congenital myopathies. Brain. 2007;130(8):2024–36. 10.1093/brain/awm096.
16. Romero NB, Monnier N, Viollet L, Cortey A, Chevallay M, Leroy JP, et al. Dominant and recessive central core disease associated with RYR1 mutations and fetal akinesia. Brain. 2003;126(Pt 11):2341–9. 10.1093/brain/awg244.
17. McKie AB, Alsaedi A, Vogt J, Stuurman KE, Weiss MM, Shakeel H, et al. Germline mutations in RYR1 are associated with foetal akinesia deformation sequence/lethal multiple pterygium syndrome. Acta Neuropathol Commun. 2014;2:148. 10.1186/s40478-014-0148-0.
18. Pergande M, Motameny S, Özdemir Ö, Kreutzer M, Wang H, Daimagüler HS, et al. The genomic and clinical landscape of fetal akinesia. Genet Med. 2020;22(3):511–23. 10.1038/s41436-019-0680-1.
19. Reischer T, Liebmann-Reindl S, Bettelheim D, Balendran-Braun S, Streubel B. Genetic diagnosis and clinical evaluation of severe fetal akinesia syndrome. Prenat Diagn. 2020;40(12):1532–9. 10.1002/pd.5809.

20. Richards S, Aziz N, Bale S, Bick D, Das S, Gastier-Foster J, et al. Standards and guidelines for the interpretation of sequence variants: a joint consensus recommendation of the American College of Medical Genetics and Genomics and the Association for Molecular Pathology. Genet Med. 2015;17(5):405–24. 10.1038/gim.2015.30.
21. Ruifrok AC, Johnston DA. Quantification of histochemical staining by color deconvolution. Anal Quant Cytol Histol. 2001;23(4):291–9.
22. Otsu N. A threshold selection method from gray-level histograms. IEEE Trans Syst Man Cybern. 1979;9(1):62–6. 10.1109/TSMC.1979.4310076.
23. Jackson M, Thomas MA, Suchet I, Mahallati H, Kuret V, Lauzon J. Lethal multiple pterygium syndrome, large cystic hygroma, and cleft palate: rare and severe fetal presentations of RYR1- and NEB-related congenital myopathies. Prenat Diagn. 2024;44(4):522–6. 10.1002/pd.6553.
24. Meier N, Bruder E, Filges I. A novel homozygous splice-site mutation in RYR1 causes fetal hydrops and affects skeletal and smooth muscle development. Prenat Diagn. 2017;37(7):720–4. 10.1002/pd.5073.
25. Hou W, Huang G, Wei H, Li W, Huang H, Qiu Y, et al. A novel homozygous intronic variant affecting splicing in the RYR1 gene contributes to fetal hydrops. Genes Dis. 2024;11(6):101375. 10.1016/j.gendis.2024.101375.
26. Bharucha-Goebel DX, Santi M, Medne L, Zukosky K, Dastgir J, Shieh PB, et al. Severe congenital RYR1-associated myopathy: the expanding clinicopathologic and genetic spectrum. Neurology. 2013;80(17):1584–9. 10.1212/WNL.0b013e3182900380.
27. Kariminejad A, Ghaderi-Sohi S, Hossein-Nejad Nedai H, Varasteh V, Moslemi AR, Tajsharghi H. Lethal multiple pterygium syndrome, the extreme end of the RYR1 spectrum. BMC Musculoskelet Disord. 2016;17:109. 10.1186/s12891-016-0947-5.
28. Zhao Q, Li X, Liu L, Zhang X, Pan X, Yao H, et al. Prenatal diagnosis identifies compound heterozygous variants in RYR1 that causes ultrasound abnormalities in a fetus. BMC Med Genomics. 2022;15:202. 10.1186/s12920-022-01358-x.
29. Alkhunaizi E, Shuster S, Shannon P, Siu VM, Darilek S, Mohila CA, et al. Homozygous/compound heterozygote RYR1 gene variants: expanding the clinical spectrum. Am J Med Genet A. 2019;179(3):386–96. 10.1002/ajmg.a.61025.
30. Wang M, Hong J, Han S, Jin P, Xu C, Qian Y, et al. Whole genome sequence identifies the second allele: an intronic variant in RYR1 contributes to early-onset fetal akinesia deformation sequence. Mol Syndromol. 2026;1–9. 10.1159/000550111.
31. Brackmann F, Türk M, Gratzki N, Rompel O, Jungbluth H, Schröder R, et al. Compound heterozygous RYR1 mutations in a preterm with arthrogryposis multiplex congenita and prenatal CNS bleeding. Neuromuscul Disord. 2018;28(1):54–8. 10.1016/j.nmd.2017.09.009.
32. Baker E, Al Gharaibeh F, Bove K, Calvo-Garcia M, Shillington A, VandenHeuvel K, et al. A novel RYR1 variant in an infant with a unique fetal presentation of central core disease. Am J Med Genet A. 2023;191(6):1646–51. 10.1002/ajmg.a.63188.
33. Casey J, Flood K, Ennis S, Doyle E, Farrell M, Lynch S. Intra-familial variability associated with recessive RYR1 mutation diagnosed prenatally by exome sequencing. Prenat Diagn. 2016;36(11):1020–6.

10.1002/pd.4925.

34. Zecevic N, Arsenijevic V, Manolakos E, Papoulidis I, Theocharis G, Sartsidis A, et al. New compound heterozygous splice site mutations of the skeletal muscle ryanodine receptor (RYR1) gene manifest fetal akinesia: a linkage with congenital myopathies. Mol Syndromol. 2020;11(2):104–9. 10.1159/000507034.
35. Xu L, Harms F, Chirasani V, Pasek D, Kortüm F, Meinecke P, et al. Single-channel properties of skeletal muscle ryanodine receptor pore Δ4923FF4924 in two brothers with a lethal form of fetal akinesia. Cell Calcium. 2020;87:102182. 10.1016/j.ceca.2020.102182.
36. Hernández-Laín A, Husson I, Monnier N, Farnoux C, Brochier G, Lacène E, et al. De novo RYR1 heterozygous mutation (I4898T) causing lethal core-rod myopathy in twins. Eur J Med Genet. 2011;54(1):29–33. 10.1016/j.ejmg.2010.09.009.
37. Suzumori N, Inagaki H, Ohtani A, Kumagai K, Takeda E, Yoshihara H, et al. Compound heterozygous RYR1 mutations by whole exome sequencing in a family with three repeated affected fetuses with fetal akinesia. Eur J Obstet Gynecol Reprod Biol. 2018;230:200–2. 10.1016/j.ejogrb.2018.09.013.
38. Ellard S, Kivuva E, Turnpenny P, Stals K, Johnson M, Xie W, et al. An exome sequencing strategy to diagnose lethal autosomal recessive disorders. Eur J Hum Genet. 2015;23(3):401–4. 10.1038/ejhg.2014.120.
39. Todd JJ, Sagar V, Lawal TA, Allen C, Razaqyar MS, Shelton MS, et al. Correlation of phenotype with genotype and protein structure in RYR1-related disorders. J Neurol. 2018;265(11):2506–24. 10.1007/s00415-018-9033-2.
40. Kushnir A, Todd JJ, Witherspoon JW, Yuan Q, Reiken S, Lin H, et al. Intracellular calcium leak as a therapeutic target for RYR1-related myopathies. Acta Neuropathol. 2020;139(6):1089–104. 10.1007/s00401-020-02150-w.
41. Iyer KA, Hu Y, Klose T, Murayama T, Samsó M. Molecular mechanism of the severe MH/CCD mutation Y522S in skeletal ryanodine receptor (RyR1) by cryo-EM. Proc Natl Acad Sci U S A. 2022;119(30):e2122140119. 10.1073/pnas.2122140119.

Figures

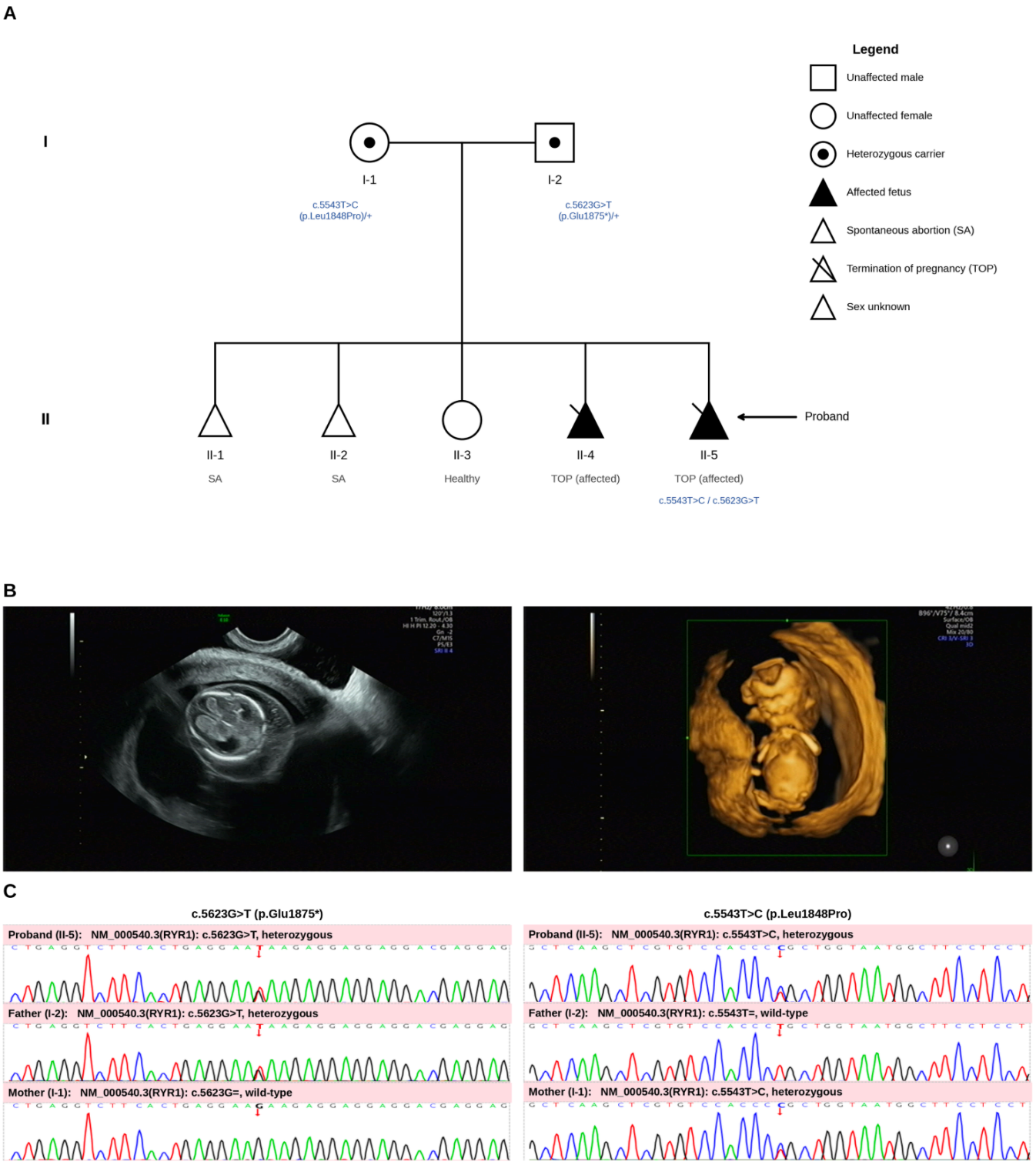


Figure 1

Clinical and genetic findings of the family. (A) Pedigree showing the proband (II-5, filled symbol) and a previously affected, terminated fetus (II-4, filled symbol); the parents are heterozygous carriers (half-filled symbols), and two spontaneous abortions (II-1, II-2) and one healthy child (II-3) are also shown. Segregation of c.5623G>T (paternal) and c.5543T>C (maternal) is indicated. (B) Prenatal ultrasound at 13+6 weeks: two-dimensional imaging showing the cystic hygroma and generalized subcutaneous edema

(left), and three-dimensional imaging showing a fixed posture of both lower limbs (right). (C) Sanger sequencing chromatograms confirming the compound heterozygous state in the proband and carrier status of each parent.

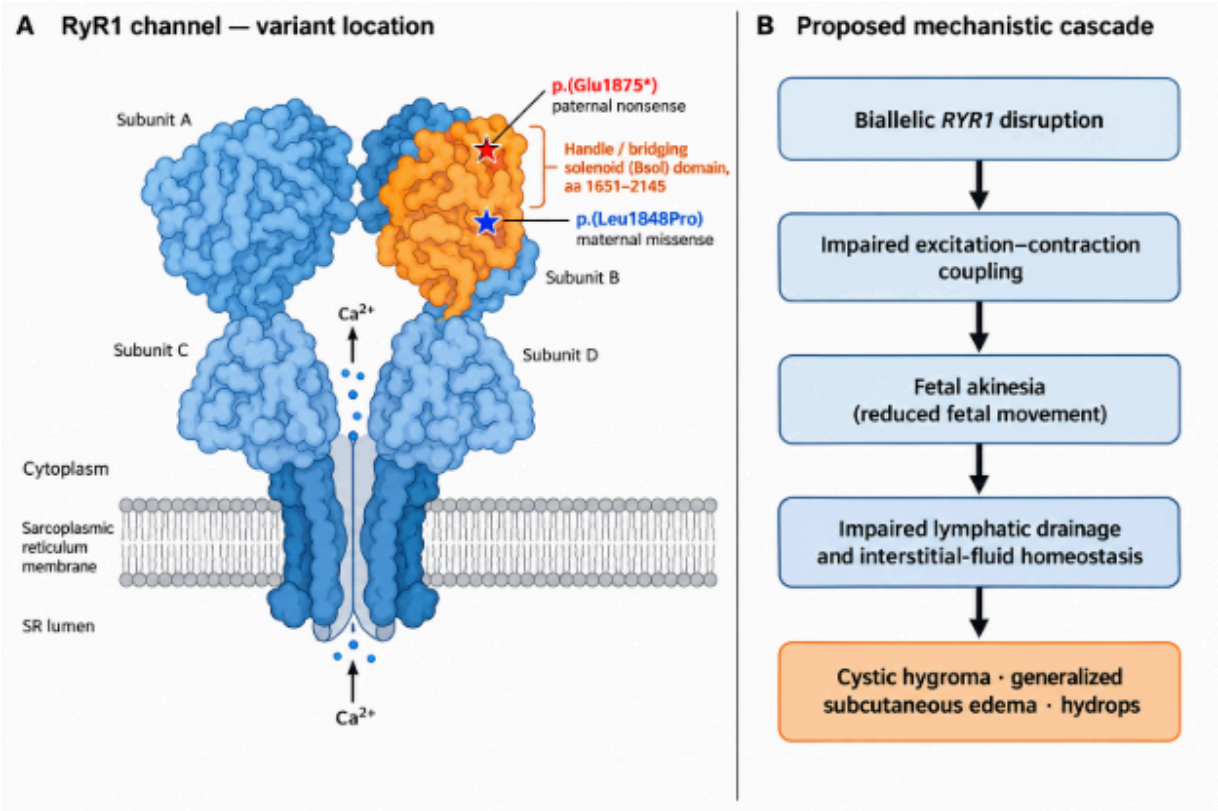


Figure 4

Proposed disease mechanism and variant locations. The diagram links biallelic *RYR1* disruption to fetal fluid accumulation and maps the present variants. Left: schematic of the RyR1 homotetramer in the sarcoplasmic-reticulum membrane; the Handle/bridging-solenoid (Bsol) domain (amino acids 1651–2145) is highlighted, and the positions of the paternal nonsense variant p.(Glu1875*) and the maternal missense variant p.(Leu1848Pro) are indicated. Right: proposed mechanistic cascade—biallelic *RYR1*disruption impairs excitation–contraction coupling, causing fetal akinesia; the resulting loss of fetal movement secondarily impairs lymphatic drainage and interstitial-fluid homeostasis, producing cystic hygroma, generalized subcutaneous edema, or hydrops. The cascade is a hypothetical disease model, not a demonstrated functional consequence of the present variants; the maternal p.(Leu1848Pro) variant remains a VUS, and biallelic *RYR1* disruption has not been established in this fetus.

Supplementary Files

This is a list of supplementary files associated with this preprint. Click to download.

- BMCMedicalGenomicsAdditionalfile1.xlsx